

The Ecology of Flows and Drift Wave Turbulence in CSDX: A Model

R. J. Hajjar,¹ P.H. Diamond,^{1,2,3} and G. R. Tynan^{1,3}

¹*Center for Energy Research, University of California San Diego, La Jolla, CA 92093, USA*

²*Center for Astrophysics and Space Sciences, University of California San Diego, La Jolla, CA 92093, USA*

³*Center for Fusion Sciences, Southwestern Institute of Physics, Chengdu, Sichuan 610041, People's Republic of China*

This paper describes the ecology of drift wave turbulence and mean flows in the coupled drift-ion acoustic wave plasma of CSDX linear device. A 1D reduced model that studies the spatiotemporal evolution of plasma mean density \bar{n} , and mean flows \bar{v}_y and \bar{v}_z , in addition to fluctuation intensity ε , is presented. Here $\varepsilon = \langle \tilde{n}^2 + (\nabla_{\perp} \tilde{\phi})^2 + \tilde{v}_z^2 \rangle$ is the conserved energy field. The model uses a mixing length l_{mix} inversely proportional to both axial and azimuthal flow shear. This form of l_{mix} closes the loop on total energy. The model self-consistently describes variations in plasma profiles, including mean flows and turbulent stresses. It investigates the energy exchange between fluctuation intensity and mean profiles via particle flux $\langle \tilde{n} \tilde{v}_x \rangle$ and Reynolds stresses $\langle \tilde{v}_x \tilde{v}_y \rangle$ and $\langle \tilde{v}_x \tilde{v}_z \rangle$. Acoustic coupling breaks parallel symmetry and generates a parallel residual stress Π_{xz}^{res} . The model uses a set of equations to explain the acceleration of \bar{v}_y and \bar{v}_z via $\Pi_{xy}^{res} \propto \nabla \bar{n}$ and $\Pi_{xz}^{res} \propto \nabla \bar{n}$. Flow dynamics in the parallel direction are related to those in the perpendicular direction through an empirical coupling constant σ_{VT} . This constant measures the degree of symmetry breaking in $\langle k_m k_z \rangle$ correlator, and determines the efficiency of $\nabla \bar{n}$ in driving \bar{v}_z . The model also establishes a relation between $\nabla \bar{v}_y$ and $\nabla \bar{v}_z$, via the ratio of the stresses Π_{xy}^{res} and Π_{xz}^{res} . When parallel to perpendicular flow coupling is weak, axial Reynolds power $P_{xz}^{Re} = -\langle \tilde{v}_x \tilde{v}_z \rangle \nabla \bar{v}_z$ is less than the azimuthal Reynolds power $P_{xy}^{Re} = -\langle \tilde{v}_x \tilde{v}_y \rangle \nabla \bar{v}_y$. The model is then reduced to a 2-field predator/prey model where \bar{v}_z is parasitic to the system and fluctuations evolve self-consistently. Finally, turbulent diffusion in CSDX follows the scaling: $D_{CSDX} = D_B \rho_{\star}^{0.6}$ where D_B is the Bohm diffusion coefficient, and ρ_{\star} is the ion gyroradius normalized to the density gradient $|\nabla \bar{n} / \bar{n}|^{-1}$.

I. INTRODUCTION

Drift wave (DW) turbulence is one of the fundamental issues in magnetically confined plasmas, and continues to be a subject of interest for many experimental and theoretical studies^{1,2}. Driven by radial inhomogeneities, drift wave fluctuations increase the turbulent transport of particles and energy, which leads ultimately to loss of the plasma particles, heat, etc. One mechanism that regulates these fluctuations is the self-generation and amplification of sheared $E \times B$ flows by turbulent stresses. This is related, but not identical to the inverse energy cascade in a two-dimensional fluid that occurs via local coupling in the wavenumber space. Here, the generation of zonal (azimuthal) flows occurs through non-local nonlinear energy transfer between the small and large scales of the plasma³⁻⁵. Such flows play an important role in saturating the drift wave instabilities, in $L - H$ transition, and in the formation of internal transport barriers (ITBs)⁶. Drift wave turbulence is also responsible for the generation of toroidal/axial flows, which play a crucial role in the macrostability of fusion grade tokamak plasmas. In particular, intrinsic toroidal flows are needed in large scale devices, where momentum input through NBI is not effective. Such flows stabilize some MHD and resistive wall modes, suppress turbulence, and enhance the overall particle confinement^{7,8}.

The relationship between drift waves and zonal flows has been extensively studied, so much so that the problem is now referred to as drift wave/zonal flow turbulence. Several self-regulating predator-prey models were developed, where the drift wave fluctuations correspond to the prey population and the zonal flows correspond to the predator population⁹⁻¹¹. As the population of drift waves grows rapidly, it supports the predator population. Zonal flows then control the drift waves by feeding on them, while being themselves regulated by a predator-prey competition and by nonlinear damping². The existing versions of these models however, do not adequately address the problem of zonal flow saturation.

In a different vein, axial flow formation by turbulence requires a breaking in parallel symmetry and a non-zero correlator $\langle k_z k_m \rangle = \sum_m k_z k_m |\tilde{\phi}|^2$. In tokamaks, it is (usually) the magnetic shear that enables the parallel symmetry breaking. In linear devices however, \mathbf{B} is constant and standard mechanisms do not apply. Recently, a parallel symmetry breaking mechanism that is based in drift wave turbulence and axial flow shear was developed¹². This mechanism does not rely on complex magnetic geometry to generate a parallel residual

stress $\Pi_{xz}^{res} \propto \langle k_z k_m \rangle$. The energy released from the density gradient is used to accelerate an axial flow through a negative viscosity process. For strong flows, the parallel shear flow instability (PSFI) controls the dynamics of \bar{v}_z .

Inverse energy cascade has been observed in both 2D and 3D systems¹³. Examples include reversal of the flux of energy in geophysical flows subject to the Earth's rotation¹⁴, as well as in shallow fluid layers¹⁵. In plasmas, inverse energy cascade that results in the generation of broadband turbulence and large scale coherent structures from DW fluctuations is widely accepted now. With drift waves triggering the formation of both axial and azimuthal flows (Fig.1), fundamental questions concerning the flow configuration arise: What mechanisms regulate the self-organization process, and ordain the final configuration of turbulence and flows in the plasma? How is energy partitioned between the fluctuations and the different flows \bar{v}_z and \bar{v}_y in the plasma? Moreover, since fluctuations and mean flows constitute an interdependent system, could there be a coupling relation between \bar{v}_y and \bar{v}_z ? If so, what determines the strength of this coupling? And most importantly, how does this coupling affect the energy branching ratio in the plasma?

To answer these questions, we present in this paper a 1D (in radius) reduced $k - \epsilon$ type model that describes the evolution of the three mean fields: density \bar{n} , axial and azimuthal flows \bar{v}_z and \bar{v}_y , as well as variations in the fluctuation intensity $\varepsilon = \langle \tilde{n}^2 + (\nabla_{\perp} \tilde{\phi})^2 + \tilde{v}_z^2 \rangle$, in the linear plasma of CSDX. The model is derived from the Hasegawa-Wakatani system with axial flow evolution included. The model self-consistently relates variations in ε to the evolution of the mean profiles via the particle flux $\langle \tilde{n} \tilde{v}_x \rangle$, and the parallel and perpendicular Reynolds stresses $\langle \tilde{v}_x \tilde{v}_z \rangle$ and $\langle \tilde{v}_x \tilde{v}_y \rangle$. Because of parallel compression, the fluctuation intensity is the relevant conserved field.

To explain the relation between \bar{v}_y and \bar{v}_z with respect to ε , the model uses a mixing length l_{mix} that reflects turbulence suppression by the axial and azimuthal flow shear. External particle and axial flow sources which result from injection of neutrals and axial momentum, are included in this model. When the work done by the fluctuations on the parallel flow is less than that done on the perpendicular flow, the model can be reduced to a 2-field predator-prey model, where the azimuthal flow feeds on the density population.

The model is a necessary intermediary between a 0D model that shows the structure of the flows and fluctuations, and a full DNS. For a multiscale system such as CSDX, a reduced model provides a route to an interpretation of the experimental results, and gives detailed

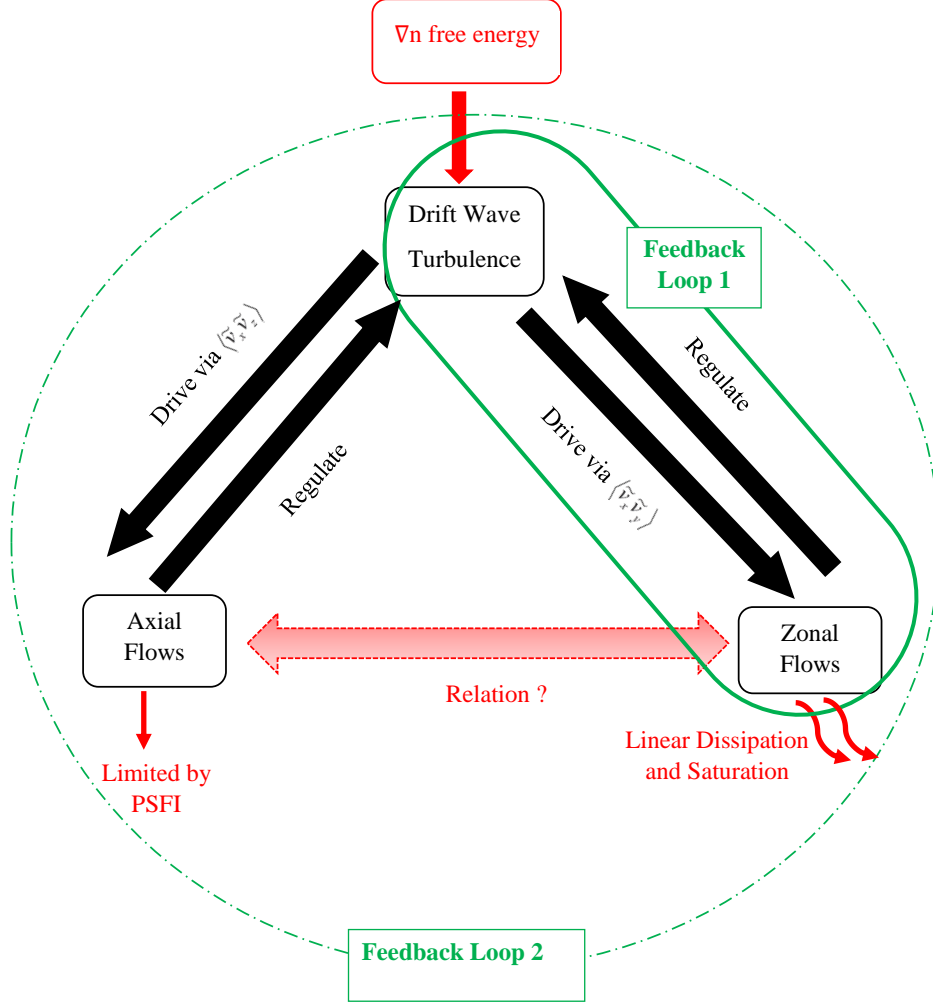


FIG. 1: A schematic of the ecology of drift wave turbulence, zonal, and axial flows. The first feedback loop relates the drift waves to the zonal flows via $\langle \tilde{v}_x \tilde{v}_y \rangle$. A second feedback loop exists as a result of a potential relation between \bar{v}_y and \bar{v}_z . The second loop relates the fluctuations to both mean flows.

insight into the feedback loops between the disparate scales. At the same time, it avoids the labor of a full DNS. The model consists of a set of compact equations that describe the evolution of the plasma stresses and flows. It shows how $\nabla \bar{n}$ free energy accelerates both \bar{v}_y and \bar{v}_z , and investigates the coupling relation between the parallel and perpendicular flow dynamics in CSDX by introducing σ_{VT} , the empirical measure of the acoustic coupling in the plasma.

The 1D reduced model description taken here should provide a useful new intermediate approach for the simulation of self-consistent evolution edge and SOL plasma profiles, transverse and parallel flows and turbulence, and would allow the study of main plasma and

trace impurity dynamics across timescales ranging from a few turbulent correlation times up to system equilibrium timescales. When modified to include toroidal and open-field line effects, and extended to a 2D geometry along the magnetic field and binormal directions, our proposed reduced model would bridge the gap between existing time-averaged fluid codes of the edge and SOL region of confinement devices (see e.g. ref.¹⁶) which are incapable of capturing such self-consistent dynamical phenomena, and fully turbulent direct numerical simulations (see e.g. refs.^{17,18}) which capture self-consistent profile and flow evolution but are computationally expensive and thus difficult to use for long time scale dynamical evolution studies. Such a new capability might be useful to study the self-consistent entrainment and transport of eroded wall impurities in flowing edge and SOL plasma and the long-time migration of these materials in the SOL and divertor regions of confinement devices. These obvious extensions are left as future work.

The rest of the paper is organized as follows. Section II presents the structure of the model, as well as a full derivation of the involved equations and an interpretation of each term of these equations. Section III elaborates on the relation between drift waves and zonal flows, and calculates the turbulent expressions for the particle flux and the vorticity flux. Expressions for the perpendicular Reynolds stress and the Reynolds work are also presented. Section IV is dedicated to the parallel Reynolds stress. This sections explains how drift waves accelerate the axial flows through $\langle \tilde{v}_x \tilde{v}_z \rangle$. An empirical constant σ_{VT} is introduced in this section. By analogy to pipe flows, σ_{VT} is presented as a measure of the acoustic coupling or the efficiency of converting the $\nabla \bar{n}$ energy to drive an axial flow. σ_{VT} is then used to establish a direct relation between the axial and the azimuthal flow shear, as both residual stresses Π_{xy}^{res} and Π_{xz}^{res} are proportional to ∇n . An expression for the mixing length l_{mix} that depends on both shears is derived in section V. In section VI, we give a summary and a discussion of the model, before reducing it to a 2-field predator-prey model in section VII. Finally, conclusion and discussion are given in section VIII.

II. THE MODEL AND ITS STRUCTURE

The basic equations are derived from the Hasegawa-Wakatani system^{19,20}, with axial flow velocity \tilde{v}_z evolution included. In a box of dimensions: $0 \leq x \leq L_x$, $0 \leq y < L_y$ and

$0 \leq z \leq L_z$, and for a straight magnetic field $\mathbf{B} = B\hat{z}$, these equations are²¹:

$$\frac{d\tilde{n}}{dt} + \mathbf{v}_E \cdot \nabla \langle n \rangle + n_0 \nabla_z \tilde{v}_z = -\frac{v_{th}^2}{\nu_{ei}} \nabla_z^2 (\tilde{\phi} - \tilde{n}) + D_0 \nabla_{\perp}^2 \tilde{n} + \{\tilde{n}, \tilde{\phi}\} \quad (1a)$$

$$\frac{d\nabla_{\perp}^2 \tilde{\phi}}{dt} + \mathbf{v}_E \cdot \nabla \langle \nabla_{\perp}^2 \phi \rangle = -\frac{v_{th}^2}{\nu_{ei}} \nabla_z^2 (\tilde{\phi} - \tilde{n}) + \mu_0 \nabla_{\perp}^4 \tilde{\phi} - \nu_{in} (\bar{v}_y - \bar{v}_n) + \{\nabla_{\perp}^2 \tilde{\phi}, \tilde{\phi}\} \quad (1b)$$

$$\frac{d\tilde{v}_z}{dt} + \mathbf{v}_E \cdot \nabla \langle v_z \rangle = -c_s^2 \nabla_z \tilde{n} + \nu_0 \nabla_{\perp}^2 \tilde{v}_z - \nu_{in} (\bar{v}_z - \bar{v}_n) + \{\tilde{v}_z, \tilde{\phi}\} \quad (1c)$$

Here x , y and z are the radial, azimuthal and axial directions respectively. The fields are normalized as follows: $\tilde{n} \equiv \tilde{n}_e/n_0$, $\tilde{\phi} \equiv e\tilde{\phi}/T_e$, $t \equiv \omega_{ci}t$, $\tilde{v}_z \equiv \tilde{v}_z/c_s$ and $length \equiv length/\rho_s$. n_0 and T_e are the average density and electron temperature respectively, $\omega_{ci} = eB/m_i$ is the ion cyclotron frequency, $c_s = \sqrt{T_e/m_i}$ is the ion sound speed and $\rho_s = c_s/\omega_{ci}$ is the ion Larmor radius with temperature T_e . v_{th} and ν_{ei} are the electron thermal velocity and the electron-ion collision frequency, respectively. The total time derivative is: $d/dt = \partial_t + \mathbf{v}_E \cdot \nabla$, and the axial ion pressure gradient is neglected in the \tilde{v}_z equation. The neutral friction, proportional to the ion-neutral collision frequency $\nu_{in} = n_n \sqrt{8T_i/\pi m_i}$, is a natural sink for energy that inverse cascades to larger scales. This friction is especially significant near the plasma boundary. Its expression can be further simplified by taking $\bar{v}_n \approx 0$ close to the boundary. Terms that are proportional to D_0 , μ_0 and ν_0 dissipate energy via viscous collisions. Finally, the nonlinear advection terms are expressed as Poisson brackets: $\{f, g\} = \partial_x f \partial_y g - \partial_x g \partial_y f$, and represent spatial scattering of fluctuations.

The system of eqs.(1) describes a variety of linearly unstable modes. One eigenmode of this system is the strongly damped ion drift wave with an eigenfrequency that satisfies the relation: $|\omega| < |k_z c_s|$. Here k_z is the parallel wave number. Such a wave is heavily damped, will be difficult to excite, and thus will not be considered here. A second solution to this system describes the dynamics of the parallel shear flow instability (PSFI). The PSFI describes turbulence production due to free energy released from parallel flow shear^{22,23}. In contrast to other linear plasmas^{24,25}, experimental results from the CSDX linear device show that the parallel flow shear \bar{v}'_z is well below the critical threshold necessary to drive PSFI²¹. The PSFI is thus heavily damped in CSDX, and will also not be considered here. A third solution describes the dynamics of the coupled 3D drift-ion acoustic turbulence. In this paper, we are mainly concerned with the coupling between the parallel and perpendicular flow dynamics. Thus we focus only on the dynamics of the coupled drift-ion acoustic waves.

We decompose each field into a mean and a fluctuating part: $f = \langle f \rangle + \tilde{f}(x, y, z, t)$, where the averaging is performed over the directions of symmetry y and z :

$$\bar{f}(x, t) = \langle f(x, t) \rangle = \frac{1}{L_z L_y} \int_0^{L_z} dz \int_0^{L_y} dy f(x, y, z, t)$$

Here we assume that the plasma profiles do not change substantially along the axial direction.

In the presence of compressible parallel flows, conservation of potential vorticity (PV) - and thus that of the potential enstrophy - is broken. Coupling between the PV fluctuations and the parallel flow compression thus defines an energy transfer channel between the parallel and perpendicular flow dynamics. This energy exchange influences the wave momentum density and modifies the zonal momentum balance theorem²⁶. In its new form, the zonal momentum balance theorem shows that coupling between drift-acoustic waves acts as a driving source that allows stationary turbulence to excite zonal flows in the absence of any driving force or potential enstrophy flux. The coupling drive involves both perpendicular and parallel dynamics, and does not require symmetry breaking in the turbulence spectrum. Therefore, instead of using potential enstrophy as the fluctuation intensity field, we use the mean fluctuation energy $\langle \varepsilon \rangle$ defined as:

$$\langle \varepsilon \rangle = \frac{1}{L_z L_y} \int_0^{L_{\parallel}} dz \int_0^{2\pi} d\theta \varepsilon(r) = \frac{1}{L_z L_y} \int_0^{L_z} dz \int_0^{L_y} dy \varepsilon(x) = \frac{\langle \tilde{n}^2 + (\nabla_{\perp} \tilde{\phi})^2 + \tilde{v}_z^2 \rangle}{2},$$

where z and y are the axial (parallel) and azimuthal (perpendicular) directions respectively, and $L_{\parallel} = L_z$ is the axial length of the plasma. Here we assume periodicity in the axial direction z . The mean fluctuating energy $\langle \varepsilon \rangle$, interpreted as a sum of internal energy $\langle \tilde{n}^2 \rangle$ and kinetic energy: $\langle (\nabla_{\perp} \tilde{\phi})^2 \rangle + \langle \tilde{v}_z^2 \rangle$, is conserved up to dissipation and internal production, as demonstrated later. The time evolution of $\langle \varepsilon \rangle$ is:

$$\frac{d\langle \varepsilon \rangle}{dt} = \frac{1}{L_z L_y} \int (\tilde{n} \frac{d\tilde{n}}{dt} + \nabla_{\perp} \tilde{\phi} \frac{d\nabla_{\perp} \tilde{\phi}}{dt} + \tilde{v}_z \frac{d\tilde{v}_z}{dt}) dy dz \quad (2)$$

An expression for eq.(2) is obtained by multiplying the set of eqs.(1) by \tilde{n} , $-\tilde{\phi}$ and \tilde{v}_z

respectively, and integrating along the directions of symmetry to get:

$$\begin{aligned}
\left\langle \frac{d\varepsilon}{dt} \right\rangle &= -\langle \tilde{n}\tilde{v}_x \rangle \frac{d\bar{n}}{dx} - \langle \tilde{v}_x\tilde{v}_y \rangle \frac{d\bar{v}_y}{dx} - \langle \tilde{v}_x\tilde{v}_z \rangle \frac{d\bar{v}_z}{dx} - \frac{1}{L_z L_y} \frac{v_{th,e}^2}{\nu_{ei}} \int \left[\partial_z(\tilde{\Phi} - \tilde{n}) \right]^2 dz - \langle \tilde{n}\tilde{v}_z \rangle \\
&\quad - \nu_{in} \left(\langle \tilde{v}_y^2 \rangle + \langle \tilde{v}_z^2 \rangle \right) - \frac{1}{L_z L_y} \int \left(D_0(\nabla_{\perp} \tilde{n})^2 + \mu_0(\nabla_{\perp}^2 \tilde{\phi})^2 + \nu_0(\nabla_{\perp} \tilde{v}_z)^2 \right) dydz \quad (3) \\
&\quad + \frac{1}{L_z L_y} \int \left(\tilde{n}\{\tilde{n}, \tilde{\phi}\} - \tilde{\phi}\{\nabla_{\perp}^2 \tilde{\phi}, \tilde{\phi}\} + \tilde{v}_z\{\tilde{v}_z, \tilde{\phi}\} \right) dydz
\end{aligned}$$

Here we have used periodic boundary conditions in the y direction to obtain the fourth term of the RHS of eq.(3). The first three terms on the RHS of eq.(3) are direct mean-fluctuation coupling terms. They relate the variations of ε to the variations of the mean profiles of \bar{n} , \bar{v}_y and \bar{v}_z via $\langle \tilde{n}\tilde{v}_x \rangle$, $\langle \tilde{v}_x\tilde{v}_y \rangle$ and $\langle \tilde{v}_x\tilde{v}_z \rangle$.

A common issue that arises while using such reduced models is the closure problem. To obtain equations that contain only the mean quantities, we simplify the energy equation by examining each term of eq.(3), in order to properly construct the equation for ε . In the case of pure drift wave turbulence, the $d\bar{v}_z/dx$ term is absent and $\omega < \omega^* \propto \nabla \bar{n}$. The density gradient term is then the only source of energy production. It is positive definite, and represents the rate at which free energy is extracted from the density gradient $\nabla \bar{n}$. The second term on the RHS of eq.(3) is the Reynolds power. It represents the free energy coupled to the azimuthal flow \bar{v}_y via the Reynolds stress $\langle \tilde{v}_x\tilde{v}_y \rangle$. For pure DWs and stable Kelvin-Helmholtz (KH) modes, this energy is transferred to the mean flow and the Reynolds power is negative. The third term, on the other hand, can represent either an energy source or an energy sink. Depending on the sign of the cross phase between \tilde{v}_x and \tilde{v}_z , this term can be either positive or negative. A detailed discussion of this cross phase relation and of the parallel Reynolds stress is deferred to a later section. The dissipation term $-\int [\partial_z(\tilde{\Phi} - \tilde{n})]^2 dz$ is associated with the phase difference between the density fluctuations \tilde{n} and the electric potential fluctuations $\tilde{\phi}$. This term is always negative. In the frequently encountered case of weakly non-adiabatic electrons, this term is always smaller than the energy input source term: $-\int [\partial_z(\tilde{\Phi} - \tilde{n})]^2 dz \ll -\langle \tilde{n}\tilde{v}_x \rangle \nabla \bar{n}^{27}$. Indeed, for $\tilde{n} = (1 - i\Delta)\tilde{\phi}$ with $\Delta \ll 1$ and $\omega \simeq |\omega^*|/(1 + k_{\perp}^2 \rho_s^2)$, the estimates of the dissipation and the energy input terms are: $\omega^2(|\omega^*| - \omega)^2$ and $\omega|\omega^*|(|\omega^*| - \omega)^2$ respectively. With $\omega < |\omega^*|$, the dissipation term can be neglected from eq.(3). The $\langle \tilde{n}\tilde{v}_z \rangle$ term represents parallel particle flux. Since such flux can be experimentally zeroed, it will be omitted from the energy equation.

Terms that are proportional to D_0 , μ_0 and ν_0 , represent collisional energy dissipation by direct energy cascade. These terms damp the fluctuation energy at small scales at a rate $\sqrt{\varepsilon}/l_{mix}$. We write the energy dissipation as $\varepsilon^{3/2}/l_{mix}$, and leave the discussion of the expression for the turbulent mixing length l_{mix} to a subsequent section. In addition to collisional dissipation, ion-neutral collisions represent a nonlinear energy damping to larger scales. Both collisional dissipation and neutral energy damping represent a sink of turbulent energy ε . Finally, the nonlinear terms in eqs. (1) are related to the $E \times B$ drift, the polarization drift, and the axial drift respectively. These terms represent the spreading of turbulence. This spreading is mesoscopic, and involves two aspects. The first aspect is a perturbation in the local intensity gradient $\partial_x \varepsilon$, i.e., a diffusion of the energy envelope to a more stable region away from its source. The second aspect includes nonlinear interaction of the local fluctuations via inverse cascade. Based in the three wave coupling, zonal flows created through inverse cascade shear the fluctuations and regulate turbulence spreading^{28,29}. We write this energy spreading as a Fickian energy flux: $\Gamma_\varepsilon = -D_\varepsilon \partial_x \varepsilon = -l_{mix} \varepsilon^{1/2} \partial_x \varepsilon$. An energy source P representing drift wave turbulent energy production is added to eq.(3). The generation of these fluctuations results from the relaxation of the mean profiles and represents the excitation in the linear phase. The energy production term is linear in ε and proportional to γ_ε , the characteristic growth rate of the DW instabilities: $P = \gamma_\varepsilon \varepsilon$. The final form of eq.(3) then becomes:

$$\frac{\partial \varepsilon}{\partial t} + \partial_x \Gamma_\varepsilon = -\langle \tilde{n} \tilde{v}_x \rangle \frac{d\bar{n}}{dx} - \langle \tilde{v}_x \tilde{v}_z \rangle \frac{d\bar{v}_z}{dx} - \langle \tilde{v}_x \tilde{v}_y \rangle \frac{d\bar{v}_y}{dx} - \frac{\varepsilon^{3/2}}{l_{mix}} + P \quad (4)$$

In addition to eq.(4), the equations for \bar{n} , \bar{v}_y and \bar{v}_z , which form the reduced model of turbulence intensity for the modified Hasegawa-Wakatani model are:

$$\frac{\partial \bar{n}}{\partial t} = -\frac{\partial}{\partial x} \langle \tilde{v}_x \tilde{n} \rangle + D_c \frac{\partial^2 \bar{n}}{\partial x^2} + S_n \quad (5)$$

$$\frac{\partial \bar{v}_z}{\partial t} = -\frac{\partial}{\partial x} \langle \tilde{v}_x \tilde{v}_z \rangle + \nu_{c,\parallel} \frac{\partial^2 \bar{v}_z}{\partial x^2} - \nu_{in} \bar{v}_z - \nu_{ii} \bar{v}_z + S_{v_z} \quad (6)$$

$$\frac{\partial \bar{v}_y}{\partial t} = -\frac{\partial}{\partial x} \langle \tilde{v}_x \tilde{v}_y \rangle + \nu_{c,\perp} \frac{\partial^2 \bar{v}_y}{\partial x^2} - \nu_{in} \bar{v}_y - \nu_{ii} \bar{v}_y + S_{v_y} \quad (7)$$

Here we assumed that the electron pressure gradient does not vary neither in the axial nor in the azimuthal direction. Note however that this assumption remains valid only in the

case of an attached plasma. When the pressure of the injected neutral gas is high enough, a detached plasma is obtained, and axial and azimuthal variations of ∇p_e are no longer equal to zero. The first terms on the RHS of eqs.(5-7) represent particle and momentum transport, while those proportional to D_c , $\nu_{c,\perp}$ and $\nu_{c,\parallel}$ represent collisional diffusivity and viscosity respectively. A particle source S_n representing the ionization of the injected neutrals is added to the density equation. Similarly, axial and azimuthal momentum sources S_{v_z} and S_{v_y} representing external input of momentum into the plasma are added to \bar{v}_y and \bar{v}_z equations. In CSDX however, no external momentum is injected and $S_{v_z} = S_{v_y} = 0$, in contrast to refs.^{22,25,30} where external axial momentum is injected into the plasma. In eq.(7), the term proportional to the ion-neutral collision frequency ν_{in} represents momentum transfer between ions and neutrals, and is significant only in the boundary layer close to the plasma wall. The last term proportional to ν_{ii} represents viscous damping via ion-ion collisions. The expressions for viscous and diffusive coefficients are³¹:

$$D_c = \frac{D}{1 + \omega_{ci}^2 \tau_i^2} \simeq \frac{D_e}{(\omega_{ci} \tau_i)^2} \sim \frac{4\sqrt{2\pi} n_0 \ln \Lambda e^2 \sqrt{m_e}}{3\sqrt{T_e}} \quad (8a)$$

$$\nu_{c,\perp} = \nu_{i,\perp} = \frac{3}{10} \frac{n_i T_i}{\omega_{ci}^2 \tau_i} \sim \frac{2\sqrt{\pi} n_0^2 \ln \Lambda e^2 m_i^{3/2}}{T_i^{1/2}} \quad (8b)$$

$$\nu_{c,\parallel} = \nu_{e,\parallel} = 0.73 n_e T_e \tau_e \sim \frac{3\sqrt{m_e} T_e^{5/2}}{4\sqrt{2\pi} \ln \Lambda e^4} \quad (8c)$$

The system formed by eqs.(4-7) conserve the total energy E_{tot} in time, up to dissipation and production. Here E_{tot} is equal to the sum of the turbulent energy ε and the mean energy $E_{mean} = (\bar{n}^2 + \bar{v}_z^2 + (\nabla_{\perp} \bar{\phi})^2)/2$. For zero energy flux conditions at the boundaries ($\partial_x \varepsilon = 0$), energy conservation (up to dissipation and production) is demonstrated as:

$$\begin{aligned} \frac{d\langle E_{tot} \rangle}{dt} &= \frac{d\langle \varepsilon \rangle}{dt} + \frac{d\langle E_{mean} \rangle}{dt} \\ &= \frac{d\langle \varepsilon \rangle}{dt} + \frac{1}{2} \frac{\partial}{\partial t} \int \left[\bar{n}^2 + \bar{v}_z^2 + (\nabla_{\perp} \bar{\phi})^2 \right] dz dy \\ &= -\langle \tilde{n} \tilde{v}_x \rangle \frac{d\bar{n}}{dx} - \langle \tilde{v}_x \tilde{v}_z \rangle \frac{d\bar{v}_z}{dx} - \langle \tilde{v}_x \tilde{v}_y \rangle \frac{d\bar{v}_y}{dx} + P - \frac{\varepsilon^{3/2}}{l_{mix}} \\ &\quad + \langle \tilde{n} \tilde{v}_x \rangle \frac{d\bar{n}}{dx} + \langle \tilde{v}_x \tilde{v}_z \rangle \frac{d\bar{v}_z}{dx} + \langle \tilde{v}_x \tilde{v}_y \rangle \frac{d\bar{v}_y}{dx} \\ &= -\frac{\varepsilon^{3/2}}{l_{mix}} + P \end{aligned} \quad (9)$$

where the order of operations $\bar{\cdot}$ and $\langle \cdot \rangle$ have been interchanged. Eqs.(4-7) thus constitute a model that describes profile evolution for both parallel and perpendicular flows, in addition to the plasma density, by self-consistently evolving turbulence as well as the mean profiles. This model offers the possibility to explain the generation and acceleration of intrinsic axial flows as a result of changes in the turbulence spectrum, governed by conservation of total energy E_{tot} .

III. CALCULATING THE TURBULENT FLUXES

Eqs.(4-7) describe time and space evolution of the three mean fields: \bar{n} , \bar{v}_y and \bar{v}_z , in addition to the mean fluctuating energy ε . The solution of this system of equations requires calculating the expressions for the different turbulent fluxes in terms of ε and the mean field gradients. In this section, we determine the expressions for the various turbulent fluxes, with the provision that these expressions are valid only in the case of nearly adiabatic electrons, that is when $k_z^2 v_{th}^2 / (\nu_{ei} |\omega|) \gg 1$. In this limit, quasi-linear theory is used to calculate the expressions for the transport fluxes by Fourier decomposing each field as: $\tilde{f}_m = \delta f_m(x) e^{i[k_m y + k_z z - \omega t]}$ where $\omega = \omega^r + i|\gamma_m|$, with $|\gamma_m| \ll \omega_m^r = \omega^*(1 + k_\perp^2 \rho_s^2)^{-1}$. Here $\omega^* = k_m v_d$, where the electron diamagnetic velocity is $v_d = -\rho_s c_s \nabla \bar{n} = \rho_s c_s / L_n$,

A. The Turbulent Particle Flux

The particle flux $\langle \tilde{n} \tilde{v}_x \rangle$ is calculated after linearizing the density equation:

$$\frac{\partial \tilde{n}}{\partial t} - \tilde{v}_x v_d + \nabla_z \tilde{v}_z = -\frac{v_{th}^2}{\nu_{ei}} \nabla_z^2 (\tilde{\phi} - \tilde{n}) + D_0 \nabla_\perp^2 \tilde{n} + \{\tilde{n}, \tilde{\phi}\} \quad (10)$$

The expression for the particle flux is then:

$$\Gamma = \langle \tilde{n} \tilde{v}_x \rangle = \sum_m \frac{v_d (\alpha + |\gamma_m|) - \alpha \omega^r / k_m}{|\omega / k_m + i\alpha / k_m|^2} |\delta \phi^2| \quad (11)$$

In the case of classic resistive drift waves, $|\gamma_m| \ll 1$ and the particle flux is:

$$\Gamma = \sum_m \alpha \frac{v_d - \omega^r / k_m}{|\omega / k_m + i\alpha / k_m|^2} |\delta \phi^2| \quad (12)$$

where $\alpha = k_z^2 v_{th}^2 / \nu_{ei}$ is the plasma adiabaticity parameter. The first term of the numerator represents diffusive relaxation of the density gradient, while the second is due to pumping by waves. The competition between these two terms is what ultimately sets the sign of Γ , i.e., the direction of the particle flux. For adiabatic electrons: $k_z^2 v_{th}^2 / \nu_{ei} \gg |\omega|$, and $\alpha \gg (\omega^r, |\gamma_m|)$. The particle flux then becomes:

$$\begin{aligned}\Gamma = \langle \tilde{n} \tilde{v}_x \rangle &= \sum_m -\frac{k_m^2 \rho_s^2 c_s^2}{\alpha} \cdot \frac{k_\perp^2 \rho_s^2}{1 + k_\perp^2 \rho_s^2} \cdot \frac{1}{n_0} \frac{d\bar{n}}{dx} \cdot |\delta\phi^2| \\ &= -D \cdot \frac{1}{n_0} \frac{d\bar{n}}{dx} > 0\end{aligned}\quad (13)$$

where the particle diffusion coefficient D is:

$$D = \sum_m \frac{k_m^2 \rho_s^2 c_s^2}{\alpha} \cdot \frac{k_\perp^2 \rho_s^2}{1 + k_\perp^2 \rho_s^2} |\delta\phi^2| = \frac{k_\perp^2 \rho_s^2}{1 + k_\perp^2 \rho_s^2} \cdot \frac{\langle \delta v_x^2 \rangle}{\alpha} \approx \frac{f\varepsilon}{\alpha}\quad (14)$$

The factor f introduced in eq.(14) represents the fraction of the fluctuation energy ε which is kinetic energy of radial motion, i.e., $f = \langle \delta v_x^2 \rangle / \varepsilon$.

1. Expression for the energy fraction f

Since the fluctuation energy ε is composed of internal energy as well as kinetic energy for both radial and axial motion, we write the following expression for the fraction of ε allocated to kinetic energy in the radial motion as:

$$f = \frac{\langle \delta v_x^2 \rangle}{\varepsilon} = \frac{\langle \delta v_x^2 \rangle}{\langle \delta n^2 \rangle + \langle \delta v_x^2 \rangle + \langle \delta v_z^2 \rangle}$$

Writing the density and radial velocity fluctuations as $\delta n = (1 - i\Delta)\delta\phi$ and $\delta v_x = -ik_\perp \rho_s c_s \delta\phi$ respectively, straightforward linearization of the axial velocity equation gives:

$$\langle \delta v_z^2 \rangle = \frac{(k_m \rho_s c_s \nabla \bar{v}_z - k_z c_s^2 (1 + \Delta^2))}{\omega^2 + 1/\tau_c^2} \langle \delta\phi^2 \rangle$$

With $\tau_c = l_{mix} / \langle \tilde{v}_x^2 \rangle^{1/2} = l_{mix} / \sqrt{f\varepsilon}$, the denominator is equal to:

$$\frac{1}{\omega^2 + 1/\tau_c^2} = \frac{l_{mix}^2 (1 + k_\perp^2 \rho_s^2)^2}{\left(l_{mix}^2 \omega^2 + f\varepsilon (1 + k_\perp^2 \rho_s^2)^2 \right)}$$

The final expression for f is:

$$f = \frac{k_{\perp}^2 \rho_s^2}{(1 + \Delta^2) + k_{\perp}^2 \rho_s^2 + \frac{|k_m \rho_s \nabla \bar{v}_z - k_z c_s (1 - i\Delta)|^2}{\omega^2 + 1/\tau_c^2}} \quad (15)$$

For adiabatic electrons and in the absence of mean axial shear ($\bar{v}'_z = 0$), f is:

$$f = \frac{k_{\perp}^2 \rho_s^2}{1 + k_{\perp}^2 \rho_s^2 + k_z^2 c_s^2 / (\omega^2 + 1/\tau_c^2)} \quad (16)$$

with $\omega = |\omega^r| = k_m \rho_s c_s / [L_n (1 + k_{\perp}^2 \rho_s^2)]$ and $1/\tau_c^2 = \varepsilon / l_{mix}^2$. In the limit of small k_z and pure DWs, eq.(16) gives: $f = k_{\perp}^2 \rho_s^2 / (1 + k_{\perp}^2 \rho_s^2) \simeq k_{\perp}^2 \rho_s^2$ and $\langle \delta v_x^2 \rangle \simeq k_{\perp}^2 \rho_s^2 \varepsilon$, as expected for adiabatic electrons.

Eq.(15) includes the correlator $\langle k_m k_z \rangle$, which expresses the cross phase relation between the velocity fluctuations in the radial direction ($\tilde{v}_x \sim k_m \tilde{\phi}$) and those in the axial direction ($\tilde{v}_z \sim k_z \tilde{p} \sim k_z T_e \tilde{n}$). Here we assumed adiabatic response with constant temperature T_e . In CSDX, the parallel to perpendicular coupling is small in comparison to $k_{\perp}^2 \rho_s^2$, as indicated by measurements of modest axial flow velocities^{32,33}. The $\langle k_m k_z \rangle$ correlator can thus be neglected in f . However, in the parallel Reynolds stress, $\langle k_m k_z \rangle$ appears as zeroth order and so cannot be dropped. Here it will be expressed in terms of an empirical constant σ_{VT} that will be introduced in a subsequent section.

B. The Vorticity Flux, the Perpendicular Reynolds Stress and the Reynolds Work

The expression for the Reynolds force needed in eq.(7) is obtained from Taylor's identity: $-\partial_x \langle \tilde{v}_x \tilde{v}_y \rangle = \langle \tilde{v}_x \nabla_{\perp}^2 \tilde{\phi} \rangle$, which relates the Reynolds force to the vorticity flux, and links the eddy fluxes of momentum and potential vorticity³⁴. When neutrals are negligible and in the presence of an externally imposed azimuthal flow V_0 , the quasi-linear expression for the

vorticity flux Π_{xy} is obtained after linearizing the vorticity equation³⁵:

$$\begin{aligned}\Pi_{xy} &= \sum_m \left\{ -|\gamma_m| \frac{v_d + d\langle \nabla_{\perp}^2 \phi \rangle / dx + V_0''}{|V_0' - \omega|^2} \right. \\ &\quad \left. + \frac{|\gamma_m| v_d + \alpha (v_d + V_0 - \omega^r / k_m)}{|\omega + i\alpha - V_0'|^2} \right\} k_m^2 \rho_s^2 c_s^2 |\delta\phi^2| \\ &= -\chi_y^{non-resonant} d(\langle \nabla_{\perp}^2 \phi \rangle + V_0') / dx + \Pi_{xy}^{res} \\ &= -\chi_y^{non-resonant} d^2(\bar{v}_y + V_0) / dx^2 + \Pi_{xy}^{res}\end{aligned}\tag{17}$$

Here $\langle \nabla_{\perp}^2 \phi \rangle$ is a self generated flow driven by the DW interaction. The expression for the vorticity flux thus consists of a residual flux Π_{xy}^{res} and a diffusive part proportional to $\chi_y^{non-resonant}$:

$$\chi_y^{non-resonant} = \sum_m \frac{|\gamma_m|}{|V_0' - \omega|^2} k_m^2 \rho_s^2 c_s^2 |\delta\phi^2|\tag{18}$$

The denominator of $\chi_y^{non-resonant}$ is a competition between the wave frequency ω and the flow shear V_0' . In CSDX, a comparison between the shearing rate V_0' and the drift wave frequency ω shows that $V_0' \ll \omega$ ³⁶. Thus we neglect the flow shear from the expression for $\chi_y^{non-resonant}$:

$$\chi_y^{non-resonant} = \sum_m \frac{|\gamma_m|}{|\omega|^2} k_m^2 \rho_s^2 c_s^2 |\delta\phi^2|$$

We also mention that the total turbulent viscosity is: $\chi_y^{tot} = \chi_y^{resonant} + \chi_y^{non-resonant}$, where $\chi_y^{resonant}$ and $\chi_y^{non-resonant}$ are the resonant and the nonresonant turbulent viscosities respectively. Here $\chi_y^{resonant} = \sum_m k_m^2 \rho_s^2 c_s^2 \pi \delta(\omega - k_m \bar{v}_y - k_z \bar{v}_z)$ results from the resonance between the plasma flows and the unstable mode of frequency ω ³⁷. Hereafter, we drop the *resonant* and *non-resonant* superscripts to simplify the notation. The residual vorticity stress Π_{xy}^{res} is:

$$\Pi_{xy}^{res} = \sum_m \left\{ \frac{|\gamma_m| v_d + \alpha (v_d - \omega^r / k_m)}{|\omega + i\alpha|^2} \right\} k_m^2 \rho_s^2 c_s^2 |\delta\phi^2| - \chi_y v_d\tag{19}$$

Note that it is through Π_{xy}^{res} that the free energy in the density gradient is converted into positive Reynolds work, resulting in the generation of flow shear. The residual stress Π_{xy}^{res} is the only term in the vorticity flux that survives when both \bar{v}_y and \bar{v}_y' vanish. Thus, it must be the case that the density gradient $\nabla \bar{n}$ accelerates the azimuthal flow from rest through

Π_{xy}^{res} . For pure Kelvin-Helmholtz modes, $k_z = \alpha = 0$ and the total stress is:

$$\Pi_{xy} = -\chi_y d\langle \nabla_{\perp}^2 \phi \rangle / dx \quad (20)$$

The residual vorticity of the pure KH modes is zero and the density gradient alone cannot drive these instabilities. KH modes simply relax the $E \times B$ flow profile via viscous diffusion. Using the expression for the particle flux, Π_{xy}^{res} is rewritten as³⁵:

$$\Pi_{xy}^{res} = \Gamma - \chi_y v_d \quad (21)$$

In the near adiabatic limit, the particle flux $\Gamma \propto 1/\alpha \ll 1$ as $\alpha \gg |\omega|$ and the residual stress is: $\Pi_{xy}^{res} = -\chi_y v_d = -\chi_y \rho_s c_s \nabla \bar{n}$. The expressions for χ_y and Π_{xy}^{res} in this limit are:

$$\begin{aligned} \chi_y &= \sum_m \frac{|\gamma_m|}{|\omega|^2} k_m^2 \rho_s^2 c_s^2 |\delta\phi^2| = \tau_c \langle \delta v_x^2 \rangle = l_{mix} \sqrt{f\varepsilon} \\ \Pi_{xy}^{res} &= -\sum_m \frac{|\gamma_m| \omega^* k_m^2 \rho_s c_s^2}{|\omega|^2} |\delta\phi^2| = -\frac{\langle \delta v_x^2 \rangle \tau_c c_s}{\rho_s L_n} = -\frac{l_{mix} \sqrt{f\varepsilon} \omega_{ci}}{L_n} \end{aligned} \quad (22)$$

where the fluctuation correlation time is $\tau_c = l_{mix} / \sqrt{f\varepsilon}$.

In addition to the Reynolds force, the expression for the local Reynolds power is needed in eq.(4). For this, we write the Reynolds stress as:

$$\langle \tilde{v}_x \tilde{v}_y \rangle = -\chi_y \frac{d\bar{v}_y}{dx} + \langle \tilde{v}_x \tilde{v}_y \rangle^{res}$$

The total Reynolds power $P_{Re} = \int (d\bar{v}_y/dx) \langle \tilde{v}_x \tilde{v}_y \rangle dV$ where $dV = dx dy dz$ can then be written as:

$$\begin{aligned} P_{Re} &= \int \frac{d\bar{v}_y}{dx} \left(-\chi_y \frac{d\bar{v}_y}{dx} + \langle \tilde{v}_x \tilde{v}_y \rangle^{res} \right) dV \\ &= \int -\chi_y \left(\frac{d\bar{v}_y}{dx} \right)^2 dV + \int \frac{d\bar{v}_y}{dx} \langle \tilde{v}_x \tilde{v}_y \rangle^{res} dV \\ &= \int \left\{ -\chi_y \left(\frac{d\bar{v}_y}{dx} \right)^2 - \bar{v}_y \partial_x \left[\langle \tilde{v}_x \tilde{v}_y \rangle^{res} \right] \right\} dV + \bar{v}_y \langle \tilde{v}_x \tilde{v}_y \rangle^{res} \Big|_{bound} \\ &= \int -\chi_y \left(\frac{d\bar{v}_y}{dx} \right)^2 dV + \int \bar{v}_y \Pi_{xy}^{res} dV \end{aligned} \quad (23)$$

Here we drop the boundary term $\bar{v}_y \langle \tilde{v}_x \tilde{v}_y \rangle^{res} \Big|_{bound}$ that results from integration by parts. We justify this by the strong neutral drag (close to the plasma boundary), so the perpendicular flow \bar{v}_y must vanish at the boundary due to no-slip condition. The local Reynolds power density is thus:

$$\langle \tilde{v}_x \tilde{v}_y \rangle \frac{d\bar{v}_y}{dx} = -\chi_y \left(\frac{d\bar{v}_y}{dx} \right)^2 + \bar{v}_y \Pi_{xy}^{res} \quad (24)$$

IV. THE PARALLEL REYNOLDS STRESS $\langle \tilde{v}_x \tilde{v}_z \rangle$

Adding axial flow to the Hasegawa-Wakatani equations breaks conservation of PV, and thus that of potential enstrophy. Moreover, it introduces an energy transfer channel between the parallel and perpendicular directions, via acoustic coupling. Experimental results show that when drift waves dominate, the turbulence production due to the release of free energy in $\nabla \bar{n}$, can excite secondary parallel flows^{22,25,30,38}. Theoretical studies also show that both axial and zonal flows are driven by turbulence, particularly by the non-diffusive residual stress in both expressions for $\langle \tilde{v}_x \tilde{v}_y \rangle$ and $\langle \tilde{v}_x \tilde{v}_z \rangle$ ^{21,23,32,39,40}. Ref.²⁶ investigates the relation between the axial and azimuthal flows and turbulence, and formulates a new zonal momentum balance theorem for the coupled drift-ion acoustic waves. Due to acoustic coupling, a dynamical mechanism for ZF generation is established. This mechanism does not require any potential vorticity flux. The sheared $E \times B$ layers so formed, break parallel symmetry (in a sheared magnetic field), generate a non-zero parallel residual stress Π_{xz}^{res} , and accelerate the axial flow \bar{v}_z , according to the mechanism of ref.⁴¹. We note, however, that strong $E \times B$ shear eventually will damp the PSFI (Fig.2). As an aside, we mention that the acceleration of zonal flows does not require external breaking of azimuthal symmetry. Zonal flows are generated by modulational instability of drift waves to a seed shear. This does not require a geometrically broken azimuthal symmetry. Axial flows on the other hand require a non-zero parallel residual stress, which can develop from a broken parallel spectral symmetry. This is one reason why zonal flows are much easier to accelerate than parallel flows. These parallel symmetry breaking mechanisms usually require the presence of a magnetic shear. However, such mechanisms are not relevant to CSDX, since \mathbf{B} is constant and magnetic shear is absent. Symmetry breaking is then provided by a dynamical mechanism, based on DWs and momentum evolution¹². The growth rate of the DWs in CSDX is determined by the frequency shift: $|\gamma| \sim \omega^* - \omega$. A test flow shear \bar{v}'_z changes this frequency shift, setting modes with

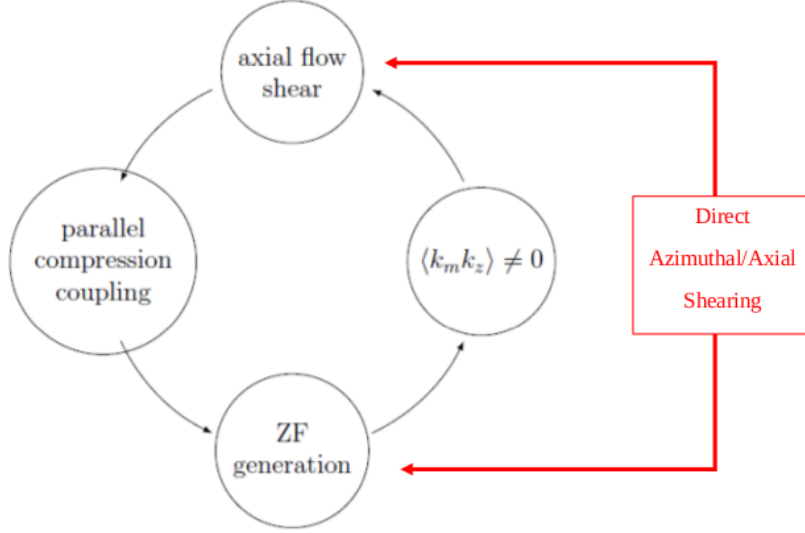


FIG. 2: Feedback loop between axial and zonal flows via $\langle k_m k_z \rangle$. A strong zonal flow shear can affect the axial flow.

$k_m k_z |\bar{v}'_z| > 0$ to grow faster than those with $k_m k_z |\bar{v}'_z| < 0$, and causing a spectral imbalance in the $k_m - k_z$ space to develop. This creates a parallel residual stress $\Pi_{xz}^{res} = -|\chi_z^{res}| \nabla \bar{v}_z$. The latter reinforces the test shear, and amplifies the parallel flow through a process of 'negative viscosity'. If \bar{v}'_z keeps increasing, the parallel shear flow instability (PSFI) will occur^{22,24}. When the PSFI is turned on, $\nabla \bar{v}_z$ saturates at the PSFI linear threshold and the total viscosity remains positive: $\chi_z^{tot} = \chi_z^{DW} + \chi_z^{PSFI} - |\chi_z^{res}| > 0$. In CSDX, no external axial momentum is injected into the plasma, and $\nabla \bar{v}_z$ never exceeds the critical value necessary to destabilize the PSFI²¹. Turbulence production thus primarily accelerates the axial flow in CSDX without destabilizing it.

A. Calculating the Expression for $\langle \tilde{v}_x \tilde{v}_z \rangle$

In the near adiabatic limit, the expression for the parallel stress $\langle \tilde{v}_x \tilde{v}_z \rangle$ is obtained by writing $\tilde{v}_x = -i k_m \rho_s c_s \tilde{\phi}$ and using eq.(1c) to get:

$$\langle \tilde{v}_x \tilde{v}_z \rangle = -\frac{|\gamma_m| \langle \delta v_x^2 \rangle}{|\omega|^2} \frac{d\bar{v}_z}{dx} + \langle k_m k_z \rangle \rho_s c_s^3 \left[\frac{|\gamma_m|}{|\omega|^2} + \frac{(\omega^* - \omega^r)}{|\omega| \alpha} \right] \quad (25)$$

In obtaining the expression for $\langle \tilde{v}_x \tilde{v}_z \rangle$, we neglected the contribution of the flow shear V'_0 with respect to the wave frequency ω , as we did in the expression for $\langle \tilde{v}_x \tilde{v}_y \rangle$. Just like χ_y ,

the total parallel diffusivity χ_z is equal to the sum of the resonant and the non-resonant part. The first component of eq.(25) is a diffusive term that is written as $-\chi_z d\bar{v}_z/dx$, where the turbulent diffusivity is:

$$\chi_z = \frac{|\gamma_m| \langle \delta v_x^2 \rangle}{|\omega|^2} = \tau_c \langle \delta v_x^2 \rangle = l_{mix} \sqrt{f\varepsilon} \quad (26)$$

We note that the turbulent parallel diffusivity χ_z given in eq.(26) is the same as the perpendicular diffusivity χ_y given in eq.(III B). The remaining part of eq.(25), involving the correlator $\langle k_m k_z \rangle = \sum k_m k_z |\delta\phi^2|$, constitutes the parallel residual stress, Π_{xz}^{res} . This term is responsible for generating the intrinsic axial flow. The expression for the parallel residual stress is:

$$\begin{aligned} \Pi_{xz}^{res} &= \sum_m \frac{|\gamma_m| k_m k_z \rho_s c_s^3}{|\omega|^2} |\delta\phi^2| + \frac{k_m k_z \rho_s c_s^3 (\omega^* - \omega^r)}{|\omega| \alpha} |\delta\phi^2| \\ &= \sum_m \frac{|\gamma_m| k_m k_z \rho_s c_s^3}{|\omega|^2} |\delta\phi^2| + \frac{k_m k_z \rho_s^3 c_s^3 k_\perp^2}{\alpha} |\delta\phi^2| \\ &= \langle k_m k_z \rangle \rho_s c_s^3 \left[\tau_c + \frac{\rho_s^2 k_\perp^2}{\alpha} \right] \end{aligned} \quad (27)$$

B. Analogy to Pipe Flow: A Simple Approach to the Physics of the $\langle k_m k_z \rangle$ Correlator

In order to calculate the parallel residual stress Π_{xz}^{res} , an expression for the correlator $\langle k_m k_z \rangle = \sum k_m k_z |\delta\phi^2|$ is needed. More importantly, in order to model the axial flow generation in CSDX, $\langle k_m k_z \rangle$ needs to be expressed in terms of a simple coefficient that can be used in numerical results. We thus draw an analogy with turbulence in a pipe flow and write \tilde{v}_z as:

$$\begin{aligned} \tilde{v}_z &= -\tilde{v}_x \tau_c \nabla \bar{v}_z + \tilde{v}^{res} \\ &= -l_{mix} \nabla \bar{v}_z + R \nabla \bar{n} \end{aligned} \quad (28)$$

The first term (proportional to $\nabla \bar{v}_z$) results from turbulent mixing on a scale l_{mix} . The second term (proportional to $\nabla \bar{n}$) relates to DWs and represents the acoustic coupling from turbulent mixing of $\nabla \bar{n}$. The latter shows how the free energy creates a residual velocity

\tilde{v}_z^{res} , (i.e., a parallel residual stress). The parallel velocity equation reads:

$$\frac{d\tilde{v}_z}{dt} = -\tilde{v}_x \frac{d\bar{v}_z}{dx} - c_s^2 \nabla_z \left[\frac{e\tilde{\phi}}{T_e} + \frac{\tilde{p}_e}{p_e} \right] \quad (29)$$

In the CSDX plasma which is nearly adiabatic and where variations of the electron temperature are negligible, we have $e\tilde{\phi}/T_e \sim \tilde{n}/\bar{n}$ and $\tilde{p}_e/p_e \sim \tilde{n}/\bar{n}$. Proceeding as for Prandtl mixing length theory, we write $\tilde{n}/\bar{n} \sim l_{mix} |\nabla \bar{n}|/\bar{n}$, and obtain:

$$\tilde{v}_z^{res} = \frac{\sigma_{VT} c_s^2 \tau_c}{L_{\parallel}} \cdot \left(-\frac{l_{mix}}{\bar{n}} \frac{d\bar{n}}{dx} \right)$$

where $L_{\parallel} = L_z$ is the axial plasma length, \bar{n} is the average plasma density and $\tau_c = l_{mix}/\tilde{v}_x$ is the fluctuation correlation time. The constant σ_{VT} is introduced as a dimensionless scaling factor between variations of \tilde{v}_z and variations of the density gradient $\nabla \bar{n}$. The final expression for \tilde{v}_z is then:

$$\tilde{v}_z = -l_{mix} \frac{d\bar{v}_z}{dx} + \frac{\sigma_{VT} c_s^2 \tau_c}{L_{\parallel}} \cdot \left(-\frac{l_{mix}}{\bar{n}} \frac{d\bar{n}}{dx} \right),$$

The parallel Reynolds stress $\langle \tilde{v}_x \tilde{v}_z \rangle$ then becomes:

$$\langle \tilde{v}_x \tilde{v}_z \rangle = -\chi_z \frac{d\bar{v}_z}{dx} - \frac{\sigma_{VT} c_s^2 \langle l_{mix}^2 \rangle}{L_{\parallel}} \cdot \frac{\nabla \bar{n}}{\bar{n}} \quad (30)$$

The first term in eq.(30) is the diagonal stress and is proportional to $\chi_z = \langle l_{mix}^2 \rangle / \tau_c$. The second term represents the parallel residual stress:

$$\Pi_{xz}^{res} = -\frac{\sigma_{VT} c_s^2 \langle l_{mix}^2 \rangle}{L_{\parallel}} \cdot \frac{\nabla \bar{n}}{\bar{n}} \quad (31)$$

The parallel Reynolds stress can then be written as:

$$\langle \tilde{v}_x \tilde{v}_z \rangle = -\chi_z \left[\frac{d\bar{v}_z}{dx} + \frac{\sigma_{VT} c_s^2 l_{mix}}{\tilde{v}_x L_{\parallel} \bar{n}} \cdot \frac{d\bar{n}}{dx} \right] \quad (32)$$

A comparison of eq.(27) and eq.(30) shows that the correlator $\langle k_m k_z \rangle$ is equal to:

$$\langle k_m k_z \rangle \left[\frac{l_{mix}}{\sqrt{f} \varepsilon} + \frac{\rho_s^2 k_{\perp}^2}{\alpha} \right] = -\frac{\sigma_{VT} \nabla \bar{n}}{\bar{n}} \cdot \frac{\langle l_{mix}^2 \rangle}{L_{\parallel} \rho_s c_s} \quad (33)$$

Eq.(33) shows that σ_{VT} is the counterpart of the correlator $\langle k_m k_z \rangle$. This constant σ_{VT} can be written as:

$$\sigma_{VT} = \frac{\langle k_m k_z \rangle}{\langle k_\perp^2 \rangle^{1/2} / L_\parallel} \quad (34)$$

where both L_\parallel and the radial wavenumber $\langle k_\perp^2 \rangle^{1/2}$ can be determined empirically. σ_{VT} captures the cross-phase information between \tilde{v}_x and \tilde{v}_z , and determines whether the parallel Reynolds power density $-\langle \tilde{v}_x \tilde{v}_z \rangle \nabla \bar{v}_z$ is an energy source or sink in eq.(4). σ_{VT} also represents the degree of symmetry breaking in the correlator $\langle k_m k_z \rangle$, and quantifies the efficiency of $\nabla \bar{n}$ in driving an axial flow. For turbulence-driven axial flows, with no axial momentum input, the parallel Reynolds stress vanishes, and the net axial flux is equal to zero: $\langle \tilde{v}_x \tilde{v}_z \rangle = 0$. The relation between the axial velocity shear and the density gradient must be:

$$\nabla \bar{v}_z = -\frac{\sigma_{VT} c_s^2 \tau_c}{L_\parallel \bar{n}} \nabla \bar{n} \quad (35)$$

Eq.(35) can be used to determine empirically the value for σ_{VT} , as τ_c is experimentally measurable.

One can also relate the variations in $\nabla \bar{v}_z$ to those in the azimuthal shear $\nabla \bar{v}_y$ via σ_{VT} . For a zero net vorticity flux: $\langle \tilde{v}_x \nabla_\perp^2 \phi \rangle = 0$, and the diffusive and the residual components of the vorticity flux are at balance:

$$\chi_y \frac{d^2 \bar{v}_y}{dx^2} = \Pi_{xy}^{res} \propto \nabla \bar{n}$$

Using eqs.(22) for χ_y and Π_{xy}^{res} in the near adiabatic limit, as well as the scaling of eq.(35), we obtain the following relation:

$$\frac{d}{dx} \nabla \bar{v}_y = \frac{\omega_{ci} L_\parallel}{\sigma_{VT} c_s^2 \tau_c} \nabla \bar{v}_z \quad (36)$$

Eq.(36) shows then how parallel and perpendicular flow dynamics are coupled. It also explains how the azimuthal shearing $\nabla \bar{v}_y$ limits the axial plasma response to the parallel residual stress Π_{xz}^{res} . As $\nabla \bar{v}_y$ increases, turbulence is suppressed, and \bar{v}_z decreases. This in turn causes σ_{VT} to decrease, thus reducing the acoustic coupling.

V. THE RADIAL MIXING LENGTH l_{mix}

A solution of the coupled drift-ion acoustic wave system requires an expression for the radial turbulent mixing length l_{mix} . In 2-D turbulent systems, the Rhines' scale, l_{Rh} , defined as the scale beyond which the inverse energy cascade terminates, emerges as an appropriate mixing length⁴². Turbulence simply changes character for $l > l_{Rh}$, and the plasma dynamics evolve from a turbulence cascade regime to wave like behavior. In CSDX, the plasma system does not exhibit a sufficiently large dynamical range of energy transfer to observe this transition in turbulence dynamics^{36,43}. Therefore, the significance of the Rhines' scale is unclear in this experiment. As mixing is regulated primarily by shearing in CSDX, a scale length that accounts for turbulence suppression due to coupling between radial fluctuations and sheared azimuthal and axial flows is suggested.

A. Case of a purely azimuthal shear

In the case of mean azimuthal shears, the following form of mixing length is suggested⁴⁴:

$$l_{mix}^2 = \frac{l_0^2}{\left[1 + (\bar{v}'_y)^2 \tau_c^2\right]^\delta} \quad (37)$$

Here δ is the suppression parameter, τ_c is the fluctuation correlation time, and l_0 is the mixing scale for turbulence in CSDX in the absence of shear flow. When the azimuthal shearing rate is greater than the fluctuations growth rate: $\bar{v}'_y > |\gamma_m|$, turbulent eddies are decorrelated and turbulence is suppressed. Coupling between the azimuthal shearing and the turbulent radial scattering of fluctuations can quench turbulence and decrease l_{mix} . An empirical relation for the scale length of turbulence $l_0 = [(\bar{k}_r^2)^{1/2}]^{-1}$ is found by expressing the inverse radial wave number k_r^{-1} as a function of the density fluctuations \tilde{n} normalized by the average plasma density \bar{n} ⁴²:

$$l_0 \simeq 2.3 \rho_s^{0.6} L_n^{0.3} \quad (38)$$

This suggests that the CSDX turbulent plasma diffusion coefficient scales like:

$$D_{CSDX} \simeq D_B \rho_\star^{0.6} \quad (39)$$

where D_B is the Bohm diffusive coefficient, and ρ_\star is the ion gyroradius normalized by the inverse density gradient scale length: $\rho_\star = \rho/L_n$. Eq.(39) suggests that the scalings of diffusion in CSDX fall in between the Bohm and gyroBohm diffusion scalings. For τ_c , we write:

$$1/\tau_c = \left(k_m^2 (v'_y)^2 \chi_y \right)^{1/3} \quad (40)$$

where the wavenumber is $k_m \simeq 1/l_0$ and the turbulent diffusivity is $\chi_y = \tau_c \langle \delta v_x^2 \rangle = \tau_c f \varepsilon$.

The correlation time is then:

$$\tau_c = \left[\frac{(v'_y)^2 f \varepsilon}{l_0^2} \right]^{-1/4}$$

and the mixing length becomes:

$$l_{mix}^2 = l_0^2 \left[1 + \frac{|v'_y| l_0}{\sqrt{f \varepsilon}} \right]^{-1} \quad (41)$$

The structure of eq.(41) shows an intuitively plausible inverse relation between the shear and the mixing length.

B. Case of azimuthal and axial shear

When both axial and azimuthal shear are present in the system, and when the azimuthal shear rate is greater than the radial correlation rate: $\bar{v}'_y > \sqrt{f \varepsilon}/l_0$, the expression for the mixing length becomes:

$$l_{mix}^2 = \frac{l_0^2}{\left[1 + \left(k_m \bar{v}'_y + k_z \bar{v}'_z \right)^2 \tau_c^2 \right]} \quad (42)$$

Here the wavenumbers can be chosen as: $k_m = 1/l_0$ and $k_z = 1/L_\parallel$. The expression for the mixing length is:

$$l_{mix}^2 = l_0^2 \left[1 + \left(\frac{\bar{v}'_y}{l_0} + \frac{\bar{v}'_z}{L_\parallel} \right)^2 \frac{l_0^2}{f \varepsilon} \right]^{-1} \quad (43)$$

The structure of eq.(43) is not significantly different from that of eq.(41). Both expressions show that l_{mix} is inversely proportional to \bar{v}'_y/\bar{v}'_z : as the shear grows, the mixing length l_{mix}

shrinks. This in turn reduces the turbulent energy ε , and increases the mean energy because of total energy conservation. In CSDX, the effective mean azimuthal shear \bar{v}'_y dominates the mean axial shear \bar{v}'_z .

VI. SUMMARY AND DISCUSSION OF THE MODEL

In summary, the model consists of the equations:

$$\frac{\partial \bar{n}}{\partial t} = -\frac{\partial}{\partial x} \langle \tilde{v}_x \tilde{n} \rangle + D_c \frac{\partial^2 \bar{n}}{\partial x^2} + S_n \quad (44a)$$

$$\frac{\partial \bar{v}_z}{\partial t} = -\frac{\partial}{\partial x} \langle \tilde{v}_x \tilde{v}_z \rangle + \nu_{c,\parallel} \frac{\partial^2 \bar{v}_z}{\partial x^2} + S_{v_z} \quad (44b)$$

$$\frac{\partial \bar{v}_y}{\partial t} = -\frac{\partial}{\partial x} \langle \tilde{v}_x \tilde{v}_y \rangle + \nu_{c,\perp} \frac{\partial^2 \bar{v}_y}{\partial x^2} - \nu_{in} (\bar{v}_y - \bar{v}_n) - \nu_{ii} \bar{v}_y + S_{v_y} \quad (44c)$$

$$\frac{\partial \varepsilon}{\partial t} - \partial_x (l_{mix} \varepsilon^{1/2} \partial_x \varepsilon) = -\langle \tilde{n} \tilde{v}_x \rangle \frac{d\bar{n}}{dx} - \langle \tilde{v}_x \tilde{v}_z \rangle \frac{d\bar{v}_z}{dx} - \langle \tilde{v}_x \tilde{v}_y \rangle \frac{d\bar{v}_y}{dx} - \frac{\varepsilon^{3/2}}{l_{mix}} + P \quad (44d)$$

The expressions for the turbulent fluxes and the Reynolds power density are:

$$\langle \tilde{n} \tilde{v}_x \rangle = -\frac{f\varepsilon}{\alpha} \cdot \frac{k_{\perp}^2 \rho_s^2}{1 + k_{\perp}^2 \rho_s^2} \cdot \frac{1}{n_0} \frac{d\bar{n}}{dx} \quad (45a)$$

$$-\frac{\partial \langle \tilde{v}_x \tilde{v}_y \rangle}{\partial x} = -l_{mix} \sqrt{f\varepsilon} \frac{d^2 \bar{v}_y}{dx^2} - \frac{l_{mix} \sqrt{f\varepsilon} \omega_{ci}}{L_n} \quad (45b)$$

$$-\langle \tilde{v}_x \tilde{v}_y \rangle \frac{d\bar{v}_y}{dx} = -l_{mix} \sqrt{f\varepsilon} \left(\frac{d\bar{v}_y}{dx} \right)^2 - \bar{v}_y \frac{l_{mix} \sqrt{f\varepsilon} \omega_{ci}}{L_n} \quad (45c)$$

$$\langle \tilde{v}_x \tilde{v}_z \rangle = -l_{mix} \sqrt{f\varepsilon} \frac{d\bar{v}_z}{dx} + \langle k_m k_z \rangle \rho_s c_s^3 \left[\frac{l_{mix}}{\sqrt{f\varepsilon}} + \frac{\rho_s^2 k_{\perp}^2}{\alpha} \right] \quad (45d)$$

$$= -l_{mix} \sqrt{f\varepsilon} \frac{d\bar{v}_z}{dx} - \frac{\sigma_{VT} c_s^2 \langle l_{mix}^2 \rangle}{L_{\parallel} L_n} \quad (45e)$$

Here l_{mix} and f are given by eq.(43) and eq.(15) respectively. The model evolves the fields \bar{n} , \bar{v}_y , \bar{v}_z and ε in space and time (x, t) using a slowly varying envelope approximation. In addition, the model self consistently relates the evolution of turbulence to that of the parallel and perpendicular flow dynamics. The coupling terms associating the turbulent energy to variations of the mean profiles \bar{n} , \bar{v}_y and \bar{v}_z , are expressed in terms of a mixing length

l_{mix} , the expression for which depends on both axial and azimuthal shear (eq.(43)). The particle flux is purely diffusive: $\langle \tilde{n}\tilde{v}_x \rangle = -D\nabla\bar{n}$. Both parallel and perpendicular Reynolds stresses consist of a diffusive part ($-\chi_z\nabla\bar{v}_z$ and $-\chi_y\nabla\bar{v}_y$), as well as a residual component proportional to $\nabla\bar{n}$ that generates an axial and an azimuthal flow.

The generated axial flow is associated with the correlator $\langle k_mk_z \rangle \neq 0$ that measures the acoustic coupling. A version of this model introduces the empirical constant σ_{VT} in the expression for $\langle k_mk_z \rangle$ (eq.(31)). This experimentally measurable constant relates the variations of the axial shear to those of the density gradient, via eq.(35). It also shows how free energy released from the density gradient can accelerate \bar{v}_z , even in the case of no axial momentum input. In addition, this constant accounts for the strength of the parallel to perpendicular flow coupling as: $\sigma_{VT} \sim \langle \tilde{v}_x\tilde{v}_z \rangle \sim \langle k_mk_z \rangle$. This coupling is stated in eq.(36), which relates \bar{v}'_z to \bar{v}'_y since both shears are dependent on the density gradient $\nabla\bar{n}$. Finally, we note that this model manifests the well known relation between turbulence and azimuthal flows via the Reynolds stress $\langle \tilde{v}_x\tilde{v}_y \rangle$ and also manifests a similar relation between fluctuations and axial flows via the parallel Reynolds stress $\langle \tilde{v}_x\tilde{v}_z \rangle$. Numerical solutions of this model will be published in a future work.

VII. REDUCING THE MODEL

When the eddy turnover time $\tau_c = l_{mix}/\tilde{v}_x$ is smaller than the confinement time $\tau_{conf} = [\bar{n}^{-1}D\nabla^2\bar{n}]^{-1}$, the model can then be reduced to a 3 field model by slaving the expression for ε to the mean profiles, and solving the equations for \bar{n} , \bar{v}_y and \bar{v}_z . Experimental results from CSDX show that the energy transfer to the axial flow via the parallel Reynolds power density: $\int -\partial_x\langle \tilde{v}_x\tilde{v}_z \rangle\bar{v}_z dx$, i.e., the power exerted by turbulence on the axial flow, is less than that exerted on the azimuthal profile via: $\int -\partial_x\langle \tilde{v}_x\tilde{v}_y \rangle\bar{v}_y dx$, by a factor of five^{32,33}. The axial flow then can be considered as parasitic to the system of $\nabla\bar{v}_y$ and $\nabla\bar{n}$. The model can be reduced even further, to 2 fields, by neglecting the axial flow equation \bar{v}_z , and solving the density and azimuthal flow equations using the stationary slaved expression for ε obtained from the equation for the mean fluctuating energy.

A. Equations and Fluxes

In this reduced model, one would still use the equations:

$$\frac{\partial \bar{n}}{\partial t} = -\frac{\partial}{\partial x} \langle \tilde{v}_x \tilde{n} \rangle + D_c \frac{\partial^2 \bar{n}}{\partial x^2} + S_n \quad (46a)$$

$$\frac{\partial \bar{v}_y}{\partial t} = -\frac{\partial}{\partial x} \langle \tilde{v}_x \tilde{v}_y \rangle + \nu_{c,\perp} \frac{\partial^2 \bar{v}_y}{\partial x^2} - \nu_{in} (\bar{v}_y - \bar{v}_n) - \nu_{ii} \bar{v}_y \quad (46b)$$

We note here that, unlike tokamaks where there is a clear scale separation: $a \geq L_n \geq l_{mix} > \rho_s$, the scale ordering in CSDX is compressed: $a > L_n \simeq l_{mix} \geq \rho_s$. Here a is the radius of the plasma. In addition, when $\sqrt{\varepsilon}/l_{mix} < (D\nabla^2 \bar{n})/\bar{n}$, a steady state solution of the energy equation generates an expression for ε , which can be used in both \bar{n} and \bar{v}_y equations. The predator-prey model thus obtained describes turbulence suppression and azimuthal flow evolution, where the flow \bar{v}_y feeds on the density gradient $\nabla \bar{n}$. An interesting feature of this model is that, unlike the model of ref.⁴⁵, the fluctuations intensity is not treated as an *ad hoc* constant, but rather evolves self consistently, albeit adiabatically (i.e. slaved to \bar{n} and \bar{v}_y). The shear $\nabla \bar{v}_y$ and $\nabla \bar{n}$ evolve in time, allowing for the level of fluctuation intensity to vary as well. In the near adiabatic electron limit, the expressions for the particle and vorticity fluxes are:

$$\Gamma = -\frac{\varepsilon f^2}{\alpha} \frac{d \ln n}{dx} = -D \frac{d \ln n}{dx} \quad (47a)$$

$$\Pi = -\sqrt{f\varepsilon} l_{mix} \frac{d^2 \bar{v}_y}{dx^2} + \frac{l_{mix} \sqrt{f\varepsilon} \omega_{ci}}{L_n} = -\chi_y \frac{d^2 \bar{v}_y}{dx^2} + \Pi^{res} \quad (47b)$$

Here $f = k_{\perp}^2 \rho_s^2 / (1 + k_{\perp}^2 \rho_s^2)$ and l_{mix} is given by eq.(41).

B. Closure by Slaving

For slaved turbulence, both the energy spreading and the energy production terms are neglected, because the eddy turnover time is shorter than the confinement time. Using eq.(24) for the Reynolds power, the fluctuation turbulent energy equation is:

$$-\Gamma_n \frac{d\bar{n}}{dx} + \chi_y \left(\frac{d\bar{v}_y}{dx} \right)^2 - \bar{v}_y \Pi^{res} - \frac{\varepsilon^{3/2}}{l_{mix}} = 0 \quad (48)$$

with χ_y and Π^{res} given above. Solution of this equation gives:

$$\varepsilon = -\rho_s^2 \left(\frac{d\bar{v}_y}{dx} \right)^2 + \frac{l_0^2}{4} \left[\frac{f^2}{\alpha} \left(\frac{dn}{dx} \right)^2 + \sqrt{\Theta} \right]^2 \quad (49)$$

where

$$\Theta = \left[\frac{f^2}{\alpha} \left(\frac{d\bar{n}}{dx} \right)^2 \right]^2 + 4f \left[\left(\frac{d\bar{v}_y}{dx} \right)^2 - \bar{v}_y \omega_{ci} \frac{d\bar{n}}{dx} \right] \quad (50)$$

One can thus use eq.(49) in the expressions for Γ and Π to close this reduced 2-field model. We note here that, in contrast to the model of ref.⁴⁵, the fluctuation level evolves in time. The reduced model then presents a coherent description of turbulence and mean profiles, without imposing a fixed level of turbulence. Solutions of this reduced model can be found by numerically solving the equations for \bar{n} and \bar{v}_y , while taking into account the corresponding expressions for l_{mix} .

VIII. CONCLUSION

This paper presents a 4-field reduced model that describes the evolution of turbulence and mean profiles in the cylindrical drift-ion acoustic plasma of CSDX. The model studies the spatiotemporal evolution of the parallel and perpendicular flow dynamics, as well as the variations of the fluctuation intensity ε . Also, the model fills the gap in approach between a 0-D 2-field reduced model (\bar{n} and \bar{v}_y), and a DNS of the three primitive equations. Moreover, this reduced model yields a better physical interpretation for the mesoscopic results observed in CSDX, while avoiding the computational cost of a full 4-field DNS.

A self-consistent description of the variations of three mean fields: density \bar{n} , azimuthal flow \bar{v}_y , and axial flow \bar{v}_z , in addition to the fluctuation intensity ε is presented here. Conservation of the total (mean + turbulent) energy, including dissipation and internal energy production, is a key element. Due to acoustic coupling, $\langle \tilde{n}^2 + (\nabla_{\perp} \tilde{\phi})^2 + \tilde{v}_z^2 \rangle$ is the conserved energy field. Because mixing occurs primarily by shearing in CSDX, the model employs a mixing length that is inversely proportional to both axial and azimuthal flow shear (eq.(43)). However, we note that in CSDX, $\bar{v}'_y > \bar{v}'_z$. The choice of a mixing length that is inversely proportional to the shear closes the loop on the total energy, and allows development of improved confinement in CSDX. Key elements of the model and its predications of experi-

mental findings are:

1. Evolution of the profiles, including mean flows and turbulent stresses, in a cylindrical plasma characterized by a constant magnetic field. The model explains how an increase in the magnitude of \mathbf{B} decreases the scale of turbulent transport and steepens the density profile. Free energy released from $\nabla\bar{n}$ accelerates then the azimuthal plasma flow \bar{v}_y , as verified experimentally³⁶. The current model is an extension of that presented in ref.⁴², where the predator/prey relation between DWs and ZFs was derived and validated.
2. In the DW dominated plasma of CSDX, a test axial flow shear breaks the parallel symmetry, which results in a residual stress $\Pi_{xz}^{res} \propto \nabla\bar{n}$ and an axial flow \bar{v}_z . Energy released from $\nabla\bar{n}$ also accelerates \bar{v}_z via the parallel Reynolds stress $\langle\tilde{v}_x\tilde{v}_z\rangle$. This trend is in agreement with the experimental results^{32,33}, and supports the analogy between the plasma and an engine³⁹. The model thus unfolds a coupling relation between \bar{v}_z and \bar{v}_y , as both flows are accelerated by the same free energy source.
3. The model reduces the evolution of plasma profiles to three fluxes: a particle diffusive flux, as well as a parallel and perpendicular Reynolds stress with residual components Π_{xz}^{res} and Π_{xy}^{res} . These fluxes regulate the transfer of energy between fluctuations and mean flows and governs the ecology of flows and drift wave turbulence.
4. The model introduces an empirical constant σ_{VT} that measures the correlator $\langle k_m k_z \rangle = \sum_m k_m k_z |\tilde{\phi}|^2$. This correlator encodes the broken symmetry of turbulence, and quantifies the efficiency of drift waves in driving Π_{xz}^{res} and \bar{v}_z through eq.(35). Because σ_{VT} measures the cross phase relation between \tilde{v}_x and \tilde{v}_z , it determines the direction of energy transfer between turbulence and axial flow.
5. Eq.(35) provides an expression for the critical density gradient necessary for onset of an axial flow shear $\nabla\bar{v}_z$. By balancing the residual and the diffusive components of the parallel Reynolds stress, we obtain:

$$\left| \frac{\nabla\bar{n}_{crit}}{\bar{n}} \right| = \frac{k_z^2 v_{th}^2}{\nu_{ei}} \frac{\omega^* L_{\parallel}}{\langle k_m k_z \rangle \rho_s c_s^3 \tau_c}$$

where τ_c is the correlation time. The model thus explains why a sheared \bar{v}_z flow was observed only above a critical \mathbf{B} value in CSDX, i.e., beyond a critical density gradient.

6. Through eq.(36), the model provides a direct expression for the parallel to perpendicular flow coupling that is reported experimentally in refs.^{32,33}. Because $\chi_y = \chi_z$, and since both Π_{xy}^{res} and Π_{xz}^{res} are proportional to $\nabla\bar{n}$, the relation:

$$\frac{d(\nabla\bar{v}_y)/dx}{\nabla\bar{v}_z} = \frac{\Pi_{xy}^{res}}{\Pi_{xz}^{res}} = \frac{\omega_{ci}L_{\parallel}}{\sigma_{VT}c_s^2\tau_c}$$

is established, and σ_{VT} is interpreted as a measure of the magnitude of coupling between $\nabla\bar{v}_y$ and $\nabla\bar{v}_z$.

7. According to eq.(39), turbulent diffusion in CSDX does not follow Bohm scaling. Scalings of turbulent diffusion in both CSDX and larger devices characterized by higher temperature follow the same trend^{46,47}

When the axial to azimuthal flow coupling is weak, the axial flow is mainly driven by the turbulent Reynolds stress, particularly by the parallel residual part. The reduced 4-field model can thus be simplified to a 2-field predator-prey model which evolves \bar{v}_y and \bar{n} . In CSDX, probe measurements show that the magnitude of \bar{v}_z is moderate, and that the parallel Reynolds power is much less than that in the perpendicular direction. Measurements also indicate a weak coupling between \bar{v}_y and \bar{v}_z ^{32,33}. This is consistent with the observation that $\nabla\bar{v}_y \ll |\omega|$ (i.e. moderate azimuthal flow) and the absence of transport barriers, because of a decoupled \bar{v}_z from \bar{v}_y . Analytically, in order to simplify the model, a slaved expression for ε is replaced in the equations for density and azimuthal flow. In contrast to the model in ref.⁴⁵ which treats the fluctuations as an *ad hoc* constant, both the fluctuations and the shear evolve in this new predator-prey model. An investigation of the numerical results obtained from such a 2-field reduced model is planned as a future work. The theory suggests the formation of zonal flows is the key part of turbulence regulation, with axial flows as parasitic. $\langle\bar{v}_x^2\rangle$ fluctuations can be determined using eq.(49), and then used to obtain $\bar{v}_z(x)$ via eq.(44b).

Future work also includes an investigation of the numerical results obtained by simulation of the reduced 4-field model, while using appropriate boundary conditions and initial profiles. These results will elucidate the details of the acceleration of axial flow, and the coupling

between \bar{v}_y and \bar{v}_z . Numerical results will also confirm the existence of a critical density gradient $\nabla\bar{n}|_{crit}$ necessary for the onset of the axial flow shear $\nabla\bar{v}_z$. The possibility of the emergence of a staircase in this 4-field model can be examined. Such crucial step is essential to understand the evolution of mesoscale structures that condense to form macroscopic barriers in the density profile.

Finally, future work in CSDX includes adding both a particle source as well as an external axial momentum source. These two sources enhance the interactions between the flows and turbulence in the plasma, leading thereby to further coupling between \bar{v}_y and \bar{v}_z according to the mechanism illustrated in fig.3. However, the azimuthal Reynolds power is much larger than the axial Reynolds power, so one may regard the axial flow evolution as parasitic to the drift wavezonal flow system. This is consistent with the observation that V moderate azimuthal flow shear) and thus there is no transport barrier.

Acknowledgments

This work was supported by the U.S. Department of Energy, Office of Science, Office of Fusion Energy Sciences, under Award Number DE-FG02-04ER54738 . The authors thank R. Hong and J. Li for useful discussions.

References

- ¹P. W. Terry. Suppression of turbulence and transport by sheared flow. *Rev. Mod. Phys.*, 72:109–165, Jan 2000.
- ²P. H. Diamond, S. I. Itoh, K. Itoh, and T. S. Hahm. Zonal flows in plasma;a review. *Plasma Physics and Controlled Fusion*, 47(5):R35–R161, 2005.
- ³W. Horton. Drift waves and transport. *Rev. Mod. Phys.*, 71:735–778, 1999.
- ⁴B. D. Scott. Energetics of the interaction between electromagnetic exb turbulence and zonal flows. *New Journal of Physics*, 7(1):92, 2005.
- ⁵P. Manz, M. Ramisch, and U. Stroth. Physical mechanism behind zonal-flow generation in drift-wave turbulence. *Phys. Rev. Lett.*, 103:165004, 2009.
- ⁶E. J. Kim and P. H. Diamond. Zonal flows and transient dynamics of the $L - H$ transition. *Phys. Rev. Lett.*, 90:185006, 2003.

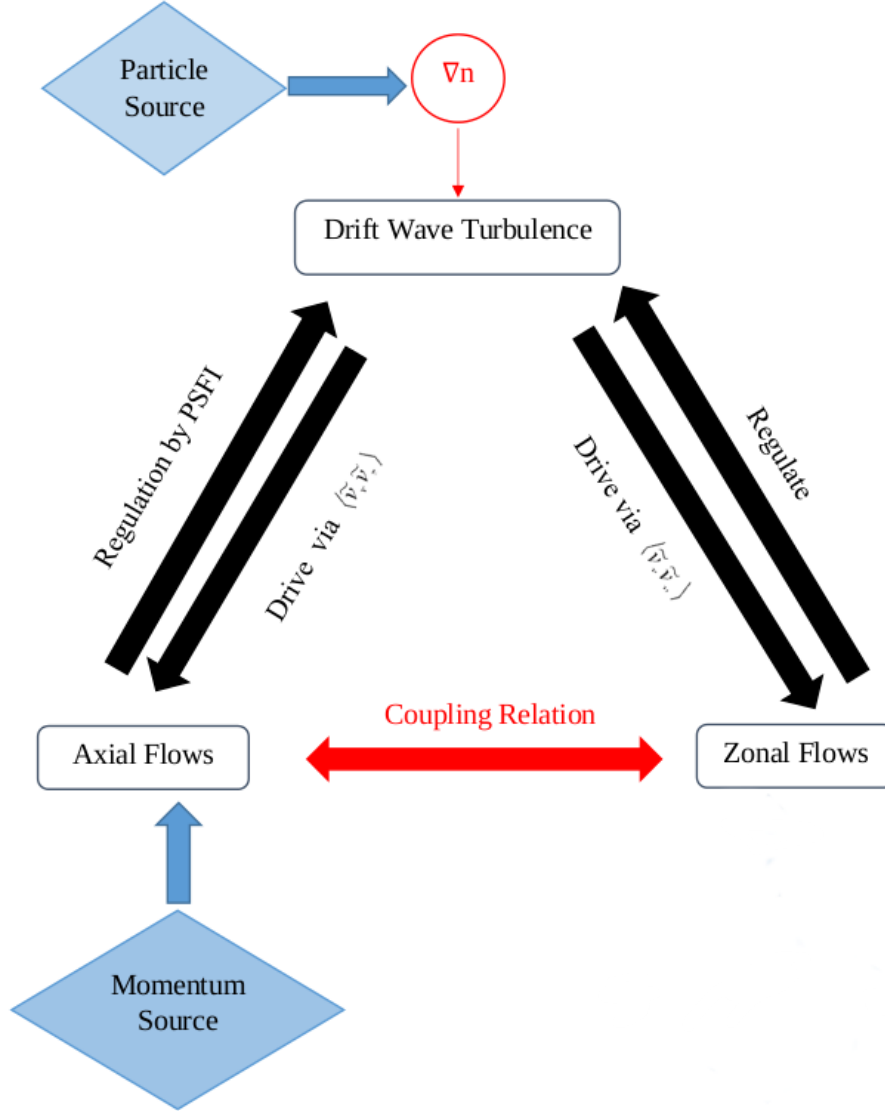


FIG. 3: The future of CSDX: particle and axial momentum sources enhance the interactions between flows and turbulence, and generate further coupling between the axial and perpendicular flow dynamics.

⁷S. S. Kim, Hogun Jhang, P.H. Diamond, L. Terzolo, S. Yi, and T.S. Hahm. Intrinsic rotation, hysteresis and back transition in reversed shear internal transport barriers. *Nuclear Fusion*, 51(7):073021, 2011.

⁸A. M. Garofalo, A. D. Turnbull, M. E. Austin, J. Bialek, M. S. Chu, K. J. Comer, E. D. Fredrickson, R. J. Groebner, R. J. La Haye, L. L. Lao, E. A. Lazarus, G. A. Navratil, T. H. Osborne, B. W. Rice, S. A. Sabbagh, J. T. Scoville, E. J. Strait, and T. S. Taylor. Direct observation of the resistive wall mode in a tokamak and its interaction with plasma rotation. *Phys. Rev. Lett.*, 82:3811–3814, 1999.

- ⁹P. H. Diamond, Y.-M. Liang, B. A. Carreras, and P. W. Terry. Self-regulating shear flow turbulence: A paradigm for the L to H transition. *Phys. Rev. Lett.*, 72:2565–2568, Apr 1994.
- ¹⁰K. Itoh and S.-I Itoh. *Plasma Phys. Control. Fusion*, 38:1, 1996.
- ¹¹K. Itoh, S. I. Itoh, A. Fukuyama, and M. Yagi. *Transport and structural formation in plasmas*. IOP, 1999.
- ¹²J. C. Li, P. H. Diamond, X. Q. Xu, and G. R. Tynan. Dynamics of intrinsic axial flows in unsheared, uniform magnetic fields. *Physics of Plasmas*, 23(5), 2016.
- ¹³Biferale L., Musacchio S., and Toschi F. Inverse energy cascade in three-dimensional isotropic turbulence. *Phys. Rev. Lett.*, 108:164501, 2012.
- ¹⁴P. D. Mininni, A. Alexakis, and A. Pouquet. Scale interactions and scaling laws in rotating flows at moderate Rossby numbers and large reynolds numbers. *Physics of Fluids*, 21(1):015108, 2009.
- ¹⁵H. Xia, D. Byrne, G. Falkovich, and M. Shats. Upscale energy transfer in thick turbulent fluid layers. *Nature Physics*, 7:321–324, 2011.
- ¹⁶S. Wiesen, D. Reiter, V. Kotov, M. Baelmans, W. Dekeyser, A.S. Kukushkin, S.W. Lisgo, R.A. Pitts, V. Rozhansky, G. Saibene, I. Veselova, and S. Voskoboinikov. The new solps-iter code package. *Journal of Nuclear Materials*, 463(Supplement C):480 – 484, 2015. PLASMA-SURFACE INTERACTIONS 21.
- ¹⁷P. Tamain, Ph. Ghendrih, E. Tsitrone, V. Grandgirard, X. Garbet, Y. Sarazin, E. Serre, G. Ciraolo, and G. Chiavassa. Tokam-3d: A 3d fluid code for transport and turbulence in the edge plasma of tokamaks. *Journal of Computational Physics*, 229(2):361 – 378, 2010.
- ¹⁸T.D. Rognlien, J.L. Milovich, M.E. Rensink, and G.D. Porter. A fully implicit, time dependent 2-D fluid code for modeling tokamak edge plasmas. *Journal of Nuclear Materials*, 196-198(Supplement C):347 – 351, 1992. Plasma-Surface Interactions in Controlled Fusion Devices.
- ¹⁹A. Hasegawa and M. Wakatani. Plasma edge turbulence. *Phys. Rev. Lett.*, 50:682, 1983.
- ²⁰A. Hasegawa and M. Wakatani. Self-organization of electrostatic turbulence in a cylindrical plasma. *Phys. Rev. Lett.*, 59:1581–1584, 1987.
- ²¹J. C. Li and P. H. Diamond. Negative viscosity from negative compressibility and axial flow shear stiffness in a straight magnetic field. *Physics of Plasmas*, 24(3):032117, 2017.

- ²²T. Kobayashi, S. Inagaki, Y. Kosuga, M. Sasaki, Y. Nagashima, T. Yamada, H. Arakawa, N. Kasuya, A. Fujisawa, S.-I. Itoh, and K. Itoh. Structure formation in parallel ion flow and density profiles by cross-ferroic turbulent transport in linear magnetized plasma. *Physics of Plasmas*, 23(10), 2016.
- ²³Y. Kosuga, S.-I. Itoh, and K. Itoh. Turbulence dynamics with the coupling of density gradient and parallel velocity gradient in the edge plasmas. *Contributions to Plasma Physics*, 56(6-8):511–515, 2016.
- ²⁴Y. Kosuga, S.-I. Itoh, and K. Itoh. Density peaking by parallel flow shear driven instability. *Plasma and Fusion Research*, 10:3401024–3401024, 2015.
- ²⁵S. Inagaki, T. Kobayashi, S. I. Itoh, T. Mitsuzono, H. Arakawa, T. Yamada, Y. Miwa, N. Kasuya, M. Sasaki, M Lesur, A. Fujisawa, and K. Itoh. A concept of cross-ferroic plasma turbulence. *Scientific Reports*, 6(22189), 2016.
- ²⁶L. Wang, P. H. Diamond, and T. S. Hahm. How does drift wave turbulence convert parallel compression into perpendicular flows? *Plasma Physics and Controlled Fusion*, 54(9):095015, 2012.
- ²⁷T. Stoltzfus-Dueck, B. D. Scott, and J. A. Krommes. Nonadiabatic electron response in the Hasegawa-Wakatani equations. *Physics of Plasmas*, 20(8):082314, 2013.
- ²⁸O. D. Gurcan, P. H. Diamond, and T. S. Hahm. Radial transport of fluctuation energy in a two-field model of drift-wave turbulence. *Physics of Plasmas*, 13(5):052306, 2006.
- ²⁹O. D. Gurcan, P. H. Diamond, and T. S. Hahm. Spatial and spectral evolution of turbulence. *Physics of Plasmas*, 14(5), 2007.
- ³⁰Y. Kosuga, S.-I. Itoh, and K. Itoh. Zonal flow generation in parallel flow shear driven turbulence. *Physics of Plasmas*, 24(3):032304, 2017.
- ³¹M. A. Lieberman and A. J. Lichtenberg. *Principles of Plasma Discharges and Materials Processing*. Wiley Interscience Publication, New York, 1994.
- ³²R. Hong, J. C. Li, S. Thakur, R. J. Hajjar, P. H. Diamond, and G. R. Tynan. Tracing the pathway from drift-wave turbulence with broken symmetry to the production of sheared axial mean flow. *submitted to Physical Review Letters*, 2017.
- ³³R. Hong, J. C. Li, R. J. Hajjar, S. Thakur, P. H. Diamond, and G. R. Tynan. Generation of parasitic axial flow by drift wave turbulence with broken symmetry: Theory and experiment. *submitted to Physics of Plasmas*, 2017.

- ³⁴G. I. Taylor. Eddy motion in the atmosphere. *Philosophical Transactions of the Royal Society of London A: Mathematical, Physical and Engineering Sciences*, 215(523-537):1–26, 1915.
- ³⁵A. Ashourvan, P. H. Diamond, and O. D. Gurcan. Transport matrix for particles and momentum in collisional drift waves turbulence in linear plasma devices. *Physics of Plasmas*, 23(2), 2016.
- ³⁶L. Cui, A. Ashourvan, S. C. Thakur, R. Hong, P. H. Diamond, and G. R. Tynan. Spontaneous profile self-organization in a simple realization of drift-wave turbulence. *Physics of Plasmas*, 23(5), 2016.
- ³⁷K. Miki and P. H. Diamond. Role of the geodesic acoustic mode shearing feedback loop in transport bifurcations and turbulence spreading. *Physics of Plasmas*, 17(3):032309, 2010.
- ³⁸S. C. Thakur, J. J. Gosselin, J. McKee, E. E. Scime, S. H. Sears, and G. R. Tynan. Development of core ion temperature gradients and edge sheared flows in a helicon plasma device investigated by laser induced fluorescence measurements. *Physics of Plasmas*, 23(8):082112, 2016.
- ³⁹Y. Kosuga, P. H. Diamond, and . D. Grcan. On the efficiency of intrinsic rotation generation in tokamaks. *Physics of Plasmas*, 17(10):102313, 2010.
- ⁴⁰P. H. Diamond, Y. Kosuga, . D. Grcan, C. J. McDevitt, T. S. Hahm, N. Fedorczak, J. E. Rice, W. X. Wang, S. Ku, J. M. Kwon, G. Dif-Pradalier, J. Abiteboul, L. Wang, W. H. Ko, Y. J. Shi, K. Ida, W. Solomon, H. Jhang, S. S. Kim, S. Yi, S. H. Ko, Y. Sarazin, R. Singh, and C. S. Chang. An overview of intrinsic torque and momentum transport bifurcations in toroidal plasmas. *Nuclear Fusion*, 53(10):104019, 2013.
- ⁴¹O. D. Gurcan, P. H. Diamond, T. S. Hahm, and R. Singh. Intrinsic rotation and electric field shear. *Physics of Plasmas*, 14(4):042306, 2007.
- ⁴²R. J. Hajjar, P. H. Diamond, A. Ashourvan, and G. R. Tynan. Modelling enhanced confinement in drift-wave turbulence. *Physics of Plasmas*, 24(6):062106, 2017.
- ⁴³P. Manz, M. Xu, S. C. Thakur, and G. R. Tynan. Nonlinear energy transfer during the transition to drift-interchange turbulence. *Plasma Physics and Controlled Fusion*, 53(9):095001, 2011.
- ⁴⁴H. Biglari, P. H. Diamond, and P. W. Terry. Influence of sheared poloidal rotation on edge turbulence. *Physics of Fluids B: Plasma Physics*, 2(1):1–4, 1990.

- ⁴⁵F. L. Hinton and G. M. Staebler. Particle and energy confinement bifurcation in tokamaks. *Physics of Fluids B: Plasma Physics*, 5(4):1281–1288, 1993.
- ⁴⁶T. Tala, C. Bourdelle, F. Imbeaux, D. Moreau, V. Parail, G. Corrigan, F. Crisanti, X. Garbet, D. Heading., E. Joffrin, L. Laborde, X. Litaudon, P. Mantica, P. Strand, and J. Weiland. Progress in transport modeling of internal transport barrier plasmas in JET. In *20th IAEA Fusion Energy Conference, Villamoura, Portugal November 1-6, IAEA*, pages Paper TH / P2-9, 2004.
- ⁴⁷P. Gohil, J. Kinsey, V. Parail, X. Litaudon, T. Fukuda, T. Hoang, for the ITPA Group on Transport, ITB Physics: J. Connor, E.J. Doyle, Yu. Esipchuk, T. Fujita, T. Fukuda, P. Gohil, J. Kinsey, S. Lebedev, X. Litaudon, V. Mukhovatov, J. Rice, E. Synakowski, K. Toi, B. Unterberg, V. Vershkov, M. Wakatani, J. Weiland, for the International ITB Database Working Group: T. Aniel, Yu.F. Baranov, E. Barbato, A. Bcoulet, C. Bourdelle, G. Bracco, R.V. Budny, P. Buratti, E.J. Doyle, L. Ericsson, Yu. Esipchuk, B. Esposito, T. Fujita, T. Fukuda, P. Gohil, C. Greenfield, M. Greenwald, T. Hahm, T. Hellsten, T. Hoang, D. Hogeweij, S. Ide, F. Imbeaux, Y. Kamada, J. Kinsey, N. Kirneva, X. Litaudon, P. Maget, A. Peeters, K. Razumova, F. Ryter, Y. Sakamoto, H. Shirai, G. Sips, T. Suzuki, E. Synakowski, and T. Takizuka. Increased understanding of the dynamics and transport in ITB plasmas from multi-machine comparisons. *Nuclear Fusion*, 43(8):708, 2003.